AGU PUBLICATIONS

JGR

Journal of Geophysical Research: Atmospheres

RESEARCH ARTICLE
10.1002/2017JD027230

**Key Points:**
- Frozen drop aggregates with similar morphology to those observed in the upper regions of thunderstorms can be produced in laboratory
- The electrical forces lead the process of collision and adhesion of frozen drops
- High concentrations of frozen drops coupled with high electrical charge appears to be the conditions for the aggregation process to occur

**Supporting Information:**
- Supporting Information S1

**Correspondence to:**
E. E. Ávila,
avila@famaf.unc.edu.ar

**Citation:**
Pedernera, D. A., & Ávila, E. E. (2018). Frozen-droplets aggregation at temperature below −40°C. *Journal of Geophysical Research: Atmospheres*, *123*. https://doi.org/10.1002/2017JD027230

Received 31 MAY 2017
Accepted 31 DEC 2017
Accepted article online 5 JAN 2018



# Frozen-Droplets Aggregation at Temperature Below −40°C

**Débora Analía Pedernera[1] and Eldo E. Ávila[1,2]**

[1]FaMAF, Universidad Nacional de Córdoba, Ciudad Universitaria, Córdoba, Argentina, [2]IFEG-CONICET, Córdoba, Argentina

**Abstract** The onset of the aggregation process of frozen droplets was investigated in laboratory settings. The experiments were conducted in a cloud chamber controlled at temperatures cooler than −40°C, where pure water droplets freeze spontaneously without the need for ice nucleating particles. We present laboratory evidence supporting that the aggregation process can occur for frozen droplet sizes around 10 μm in diameter and at concentrations observed in the cloud chamber of 70 ± 20 $cm^{-3}$, which can be found in some regions of anvil cirrus. The characteristics and morphology of the aggregates were examined in detail. Additional experiments performed with electrically charged droplets show that the aggregation processes can be significantly accelerated, suggesting that the mechanism of collision and adhesion could be related to electrical forces generated by different charge distributions or dipole interactions between the interacting ice surfaces. The current work aims at advancing our fundamental understanding of the aggregation process of frozen droplets, which is necessary for understanding the cloud microphysical processes.

## 1. Introduction

Jensen et al. (2009) and Lawson et al. (2010) show measurements of small ice particles reaching concentrations of tens per $cm^{-3}$ near convective turrets in anvil cirrus. These particles can absorb/emit infrared thermal radiation and absorb/scatter solar radiation; thereby, they play a key role in the radiative energy budget of the Earth (Liou, 1986; Lynch et al., 2002).

Vigorous continental convective storms can generate anvil cirrus that resides high in the troposphere (Salby et al., 1991; Sassen et al., 2008). There is observational evidence that homogeneous nucleation in deep convection may be a significant source of frozen droplets to the upper levels of the troposphere (Heymsfield et al., 2009; Lawson et al., 2010; Rosenfeld & Woodley, 2000). In fact, the supercooled cloud droplets are lifted in strong updrafts and frozen when they reach heights above the −38°C isotherm.

There is extensive evidence that homogeneous nucleation in deep convection could produce high concentration of frozen droplets in clouds, which could lead to the formation of aggregates of frozen droplets. Gayet et al. (2012) reported unusually high values of ice particle concentrations (up to 70 $cm^{-3}$) near the top (~11,000 m) of an overshooting convective cell over continental areas in Europe, which confirms the availability of cloud droplets to be carried up to regions colder than −38°C.

The aggregation process involves collision and adhesion of ice particles and produces an enhancement of the growth rates and sedimentation of the particles.

Early in the second half of the last century, it was thought that the aggregation process could only occur at temperatures above −25°C. Hosler et al. (1957) studied experimentally the aggregation of ice crystals colliding with an ice sphere and found that at ice saturation no aggregation occurred at temperatures below −25°C. Hobbs and Mason (1964) made a study of aggregation of single crystal and polycrystalline ice spheres. They used particles of 50–700 μm in diameter, and a temperature range of −3 to −20°C, in air at atmospheric pressure. They suggested that the growth of the initial neck, formed in the contact area, is controlled by the vapor supply from areas close to the neck and concluded that vapor transport is the dominant mechanism. However, Kikuchi (1972) analyzed the rate of growth of the ice neck between natural aggregated frozen cloud particles and concluded that the aggregation mechanism was not only by evaporation-condensation but also by volume diffusion and plastic or viscous flow.

In situ studies have reported observations of aggregation of ice particles at temperatures colder than −25°C. Thuman and Robinson (1954) collected ice fog particles in the Fairbanks area, Alaska. Microscopic

examination of the slides collected in this study showed aggregation of quasi-spherical droxtals with a mean diameter of 13 μm, at surface temperatures around −40°C. Kumai (1966) showed examples of aggregation of two natural ice fog crystals of 10 μm diameter at air temperature around −40°C observed in Fairbanks. Kikuchi (1972) reported photographs of sintered frozen cloud particles observed at around −25°C in Syowa Station, Antarctica.

However, Schmitt et al. (2013) carefully observed that there was no aggregation in the free atmosphere in polar regions. They studied the microphysical properties of ice fogs measured in the Fairbanks region at −30°C and colder and found that most of the observed particles smaller than 10 μm were quasi-spherical droxtals and noted that the droxtals aggregation observed in the images were not aggregated in the air but came into contact after collection. These results suggest that the previous observations of aggregation in polar regions were probably the result of particles falling on top of one another.

Heymsfield (1986) and Kajikawa and Heymsfield (1989) observed aggregation of ice crystals in cirrus at temperatures between −30°C and −45°C. More recently, Lawson et al. (2003), Connolly et al. (2005), Gayet et al. (2012), and Stith et al. (2014), using aircraft instrumentation, observed chains of frozen droplets in several locations and also found evidence that the aggregation process can occur at temperatures of −40°C and below.

Latham and Saunders (1967) measured the force required to separate two ice spheres in the presence of an external electric field ($E$). They found that the force increased rapidly with increasing $E$ and suggested that the rate of growth of snowflakes in a cloud by means of ice crystal aggregation can be markedly enhanced if the cloud is highly electrified. It was hypothesized that the aggregation processes occurring at low temperatures is due to electrical forces in the clouds (Connolly et al., 2005; Lawson et al., 2003). However, the primary mechanism to explain aggregation process and its link with electrical forces has not been elucidated yet.

Here we present new laboratory results, which extend the number of observations of frozen droplets aggregates for temperatures $<-40$°C. In this work, the onset of the aggregation process of frozen droplets was closely examined and analyzed for the purpose of inferring the controlling factors in the processes. The knowledge of the aggregation processes of frozen droplets is necessary for understanding the cloud microphysical processes.

Laboratory studies have the great advantage of being able to control and characterize the environmental conditions, under which the experiments are performed. In addition, the processes on the scale of the tens of microns can be discerned in good detail, which is very difficult for the instruments used for airborne, in situ measurements.

## 2. Experimental Method

The current set of experiments was carried out in the Atmospheric Physics Laboratory of the University of Córdoba, Argentina, where the altitude is ~470 m above sea level. The tests were conducted in a thermostated cloud chamber of 170 L of capacity with temperature control down to −50°C and at atmospheric pressure.

A cloud of water droplets was generated outside the cloud chamber by condensation of water vapor, provided by a boiler connected to a controlled power output. This vapor creates the cloud of water droplets, which is conducted into the chamber. The water used in all experiments was prepared from a Milli-Q. After being introduced, the droplets reach the temperature of the chamber ($<-40$°C) and then they spontaneously begin the freezing process until the drop is completely solidified. It can be estimated that the thermalization and freezing times for a droplet of 10 μm in diameter are around $10^{-6}$ s and $10^{-3}$ s, respectively (Johnson & Hallett, 1968). Thus, for all practical purposes it can be assumed that an ice cloud is immediately formed after the droplets are introduced inside the chamber. Controlling the injection time, it is possible to control the cloud density in the chamber. A thermometer was fixed to continuously monitor ambient temperature inside the cloud chamber. Initially, the droplets were generated outside the cloud chamber in order to be sure that we work with liquid droplets that subsequently freeze upon entering the chamber at temperatures $<-40$°C. Otherwise, if the vapor is introduced directly into the chamber, ice particles could form without passing through the liquid phase, and they do not hold the typical spherical shape of the frozen droplets that we want to analyze.

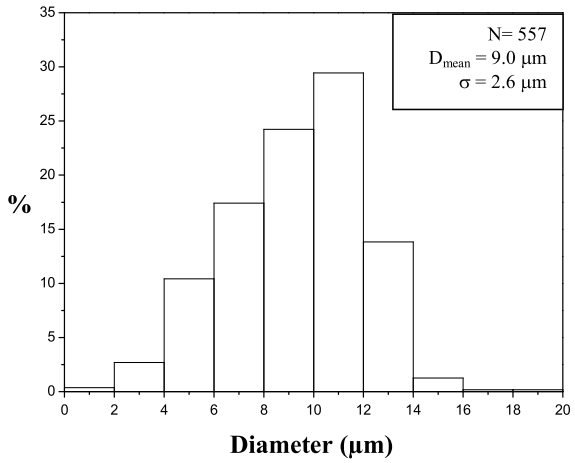


**Figure 1.** Size distribution of cloud droplets formed by condensation of water vapor.

Samples of the ice cloud were obtained at different times by taking plastic replicas of the cloud with a glass microscope slide (Schaefer, 1956). In this technique, the particles are allowed to immerse into a solution of polyvinyl formal resin (Formvar) dissolved in a solvent (chloroform). The solvent then evaporates leaving the ice particles encased in the plastic film. The ice particles evaporate through the film leaving hollow plastic replicas, which exactly reproduce the shape and size of the original particles. These replicas can then be examined under microscope at room temperature and digital images are taken with a digital camera. The collection was performed by pumping out 4 L air volume from the chamber into the coated glass slide. The smallest particle size that can be identified with this technique is ~2 μm.

## 3. Results and Discussion

Plastic replicas were taken before the injection of the cloud droplets in order to check the absence of spurious particles inside the chamber. Each test lasted approximately 6 min, and the cloud was sampled in intervals of about 1 min.

The droplet sizes ranged from 2 to 20 μm, while the average diameter and the standard deviation were 9.0 μm and 2.6 μm, respectively. Figure 1 displays the histogram of the droplet size distribution; the single frozen droplets on the plastic replicas were measured to build the histogram. This spectrum shows that the droplets used in this study could be representative of those found in real clouds (Rosenfeld et al., 2006).

Besides the frozen droplets with the typical spherical shape, it was observed that the ice cloud samples also included some irregular-shaped particles. Likely, the irregular particles belong to ice particles grown directly from the vapor phase on ice nucleating particles (INPs), that is, through the deposition nucleation mechanism. During the experiments, natural INPs can be activated due to the vapor pressure is raised due to warm humid air (at ambient temperature) enters into the chamber together with the droplet cloud.

Figure 2 shows the photographs of typical ice particles found on the replicas belonging to an experiment carried out at $T = -(46 \pm 1)$°C. In the figure it is possible to identify the following varieties of ice particles: single frozen droplets, ice crystals grown by vapor deposition, droplet-droplet aggregates, crystal-droplet aggregates, and crystal-crystal aggregates. A photograph of a circular region of the replica with typical ice particles found in the above mentioned experiment can be observed in Figure 2a. Single frozen droplets, some of them with a smooth spherical surface, the other ones with protuberances on their surfaces, can be seen in Figure 2b. Pure aggregates of single frozen droplets, most of them composed of two or three frozen droplets, are shown in Figure 2c. Ice particles like hexagonal plates, columnar ice crystals, dendrites and sector plates, and other asymmetric ice particles are observed in Figure 2d. Pure aggregates of ice particles mentioned in Figure 2d are shown in Figure 2e. Finally, mixed aggregates of single frozen droplets with particles mentioned in Figure 2d can be seen in Figure 2f.

The particles shown in Figure 2 were sampled 60 s after the cloud injection. In general, we observe that the number of aggregated particles is incremented with time, as well as the number of the aggregates with more than two droplets increases with time. Nevertheless, we cannot rigorously study the temporal evolution of the droplet population because the larger particles rapidly fall to the floor of the chamber.

The particle concentration was estimated quantitatively by passing a known volume of the cloud over the glass slide. The concentration during this experiment was estimated at $(70 \pm 20)10^3$ particles $L^{-1}$, which belongs to an ice water content ~0.03 g $m^{-3}$. These estimates consider a monodisperse particle size distribution with diameter equal to the average diameter shown in Figure 1. Higher values of the concentration of small ice particles were found near the top of convective cells when compared with values of cirrus at similar temperatures. For instance, Gayet et al. (2012) reported concentrations of small ice particles between (20 and 70) $\times$ $10^3$ $L^{-1}$ in overshooting convective cells for temperatures around $-50$°C, while the concentration within surrounding cirrus cloud was ~6 $\times$ $10^3$ $L^{-1}$. Concentrations of small ice particles between (50 and 100) $\times$ $10^3$ $L^{-1}$ have been also measured near the top of tropical convection by Knollenberg et al. (1993)

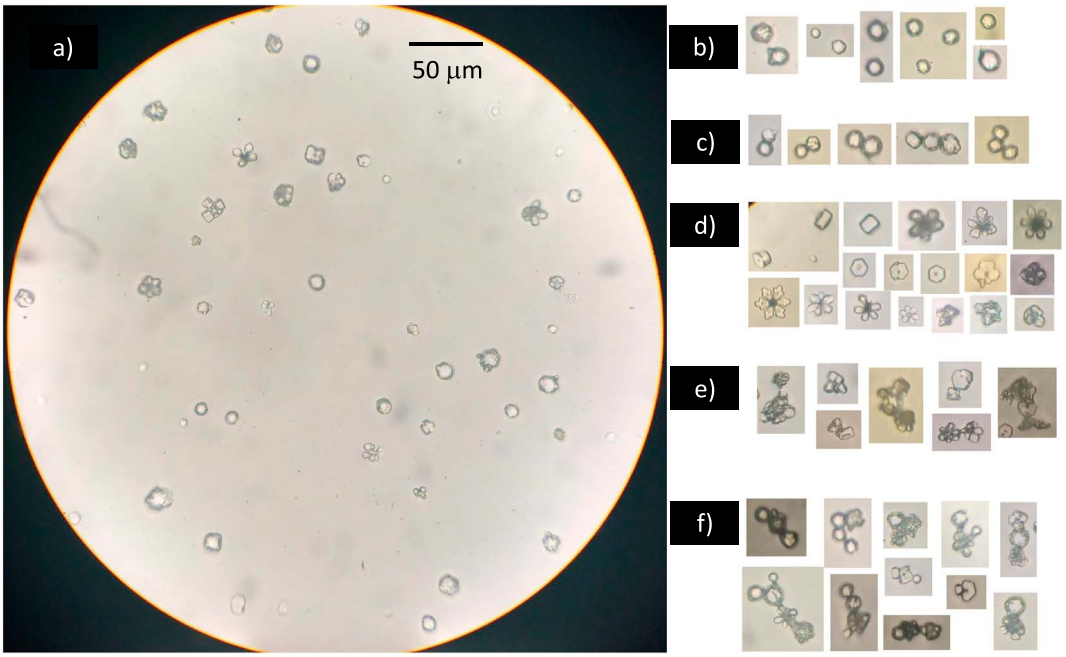


**Figure 2.** Examples of ice particles captured during an experiment at $T = -(46 \pm 1)$°C. (a) A typical photograph of the collected sample. (b) Single frozen droplets. (c) Droplet-droplet aggregates. (d) Ice crystals grown by vapor deposition. (e) Crystal-crystal aggregates. (f) Crystal-droplet aggregates.

and Heymsfield et al. (2005, 2006). The ice particle concentrations used in this work are higher but of the same order of magnitude as found in anvil cirrus, but not in synoptic cirrus.

It is important to remark that practically in all the aggregated particles observed on the Formvar samples, the contact occurs on the surfaces of each one of the involved droplets. Superimposed droplets are not observed as would be expected in the case in which they were coupled after collection of particles on the Formvar. This is a clear indication that the frozen droplets do aggregate in the free air and do not come into contact after collection as noted by Schmitt et al. (2013) in ice fogs measured in the Fairbanks.

In the case that the droplet number concentration is incremented, the number of collisions between the frozen droplets is expected to increase; thereby, aggregates with larger droplet number and more complex particle shapes should appear with a larger frequency. Figure 3 shows the photographs of different types of aggregates found for an experiment where the droplet number concentration was deliberately incremented by almost one order of magnitude [$\sim(50 \pm 20)10^4$ $L^{-1}$] with respect to the previous measurement. The run was performed at $T = -(43 \pm 1)$°C. The varieties and morphologies of the frozen droplet aggregates found in this experiment were similar to the CPI images of particles encountered by Connolly et al. (2005) and Stith et al. (2014) and displayed by Stith et al. in their Figures 5–7 and 14. According to their classification of aggregates, simple forms, primary linear chains, heavily branched, and internally mixed aggregates could be sampled and identified in the above mentioned experiment of the present work, and they are shown in the Figure 3. These results suggest that the concentration of particles is a very relevant factor for the formation of aggregates that explains why aggregation of small frozen drops and ice crystals is mainly found in the tops of continental thunderstorms (Connolly et al., 2005; Lawson et al., 2003).

In order to study the physical mechanism responsible for the aggregation process, another cloud production method was used. The water droplet cloud was now generated from an ultrasonic nebulizer. Electrical charge is separated when a liquid surface is disrupted by nebulization, so that electrically charged water droplets were generated by using typical clinical nebulizers (Bailey et al., 1998; Saini et al., 2007). This observation is generally supported by our earlier measurements. In fact, we have performed laboratory experiments where simulated graupel pellets were grown by accretion or riming of supercooled water drops. Riming occurred on a fixed collector of millimeter size, which is connected to a sensitive current amplifier capable of detecting

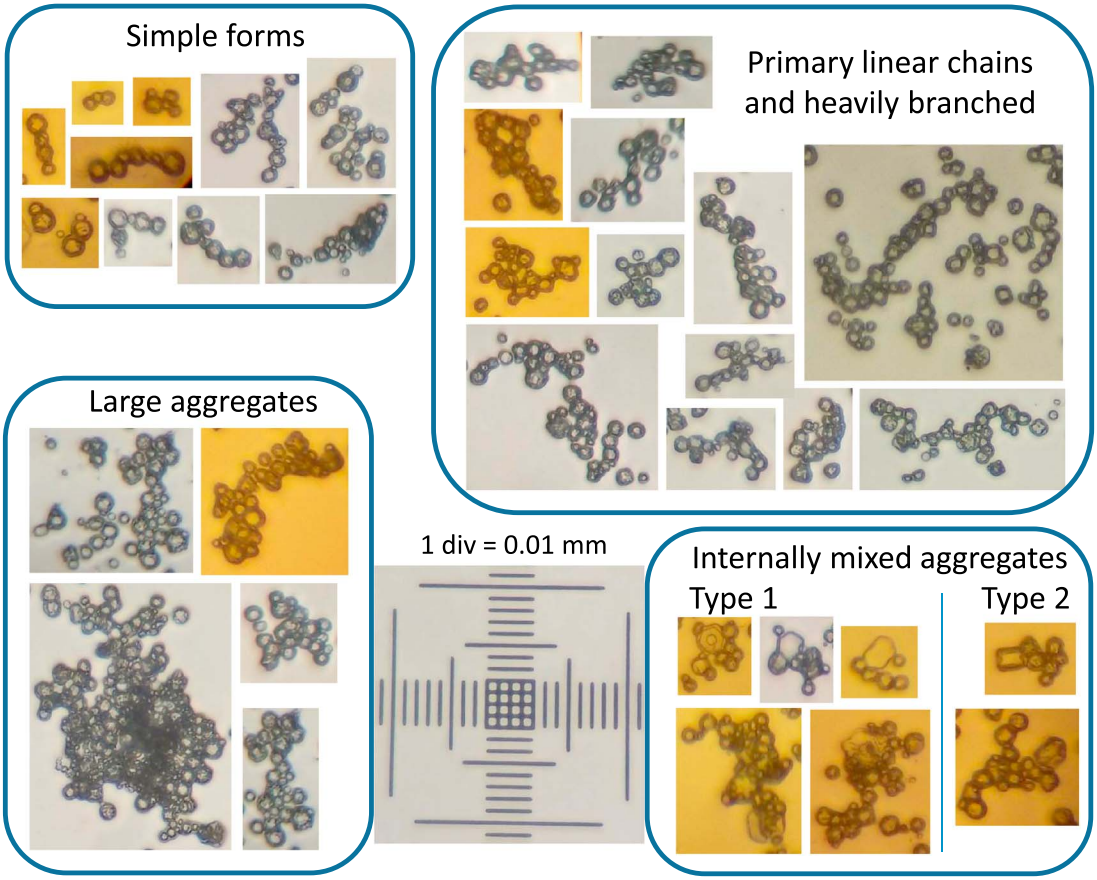


**Figure 3.** Images of chain aggregates found for a measurement performed at $T = -(43 \pm 1)$°C and droplet concentration ~$(50 \pm 20)10^4$ particles $L^{-1}$.

electrical currents larger than 1 pA. We observed that the accretions of supercooled water droplets generated by nebulizers produce an oscillating electric current and an increment of the electric noise. On the other hand, the accretions of supercooled water droplets generated by condensation do not produce electric current nor electric noise on the collector. The occurrence of the electric noise and oscillating current is a clear indication that the droplets generated by the nebulizers are charged with both signs. However, in those experiments we did not measure the magnitude of the charge carried by individual droplets, so that we appeal to data from the literature, which unfortunately are very scarce. Chow and Mercer (1971) measured the charges on droplets produced by atomization for different concentration of sodium chloride-uranine solute in water (0.1%, 1.0%, and 10%). They showed that the number of elementary charges on the droplets depends on the droplet size and for a concentration of 0.1% they found that the number of elementary charges on the droplets ($n$) can be estimated as $n = 4.8d^{0.6}$ where $d$ is particle diameter in microns. They estimated that about 20 elementary charges can be carried per droplet up to 10 μm in diameter; the droplets can carry charges of both signs. This result is not directly applicable to the current results because the nebulizer was used with pure water (Milli-Q), but it could give an idea of the order of magnitude of the charge per droplet. For comparison with droplets formed by condensation, Allee and Philips (1959) measured the cloud droplet charge in natural supercooled clouds, and they found that droplets of 10 μm in diameter carried in average five elementary charges per droplet, being the charge distribution symmetric about zero charge.

Thus, the effect of the presence of electrically charged droplets on the aggregation process was analyzed. Figure 4 displays the droplet size distribution of the cloud generated by the nebulizer. The water droplet sizes ranged from 2 to 16 μm, while the average diameter and the standard deviation were 7.4 μm and 2.1 μm, respectively. Figure 5 shows pictures of the particles found on the replicas belonging to an experiment

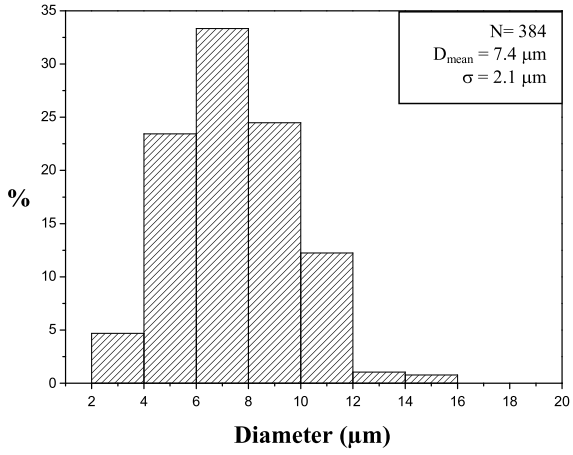


**Figure 4.** Size distribution of cloud droplets formed by ultrasonic nebulizer.

carried out with a cloud droplet generated with a nebulizer at $T = -(43 \pm 1)$°C. The particle concentration during this experiment was estimated as $(60 \pm 20)10^3$ particles $L^{-1}$.

Table 1 displays the results obtained in experiments working with the ultrasonic nebulizer and with water condensation. The table lists the temperature range, the initial concentration of frozen droplets ($C_o$), the number of single frozen droplets and the number of aggregates with 2, 3, 4, and >4 frozen droplets counted in each experiment. Only single frozen droplets and droplet-droplet aggregates were considered in this analysis. It can be observed that in the experiment working with the ultrasonic nebulizer, the ratio between the total number of aggregates (two or more frozen droplets, $N_a$) to the number of single frozen droplets ($N_{sd}$) is significantly higher than in the case without nebulizer. In fact, $N_a/N_{sd} \sim 0.32$ in the case with nebulizer and $N_a/N_{na} \sim 0.07$ in the case without nebulizer. It is plausible to assume that the enhanced ability for aggregation is due to the effect of the electrical charge carried by the droplets generated by the nebulizer. Ice consists of polar water molecules that can interact with other substances containing polar molecules. There is theoretical and experimental evidence about the existence of a surface charge on ice; this surface charge can interact with another surface; particularly, it is reasonable to assume that two charged surfaces can generate electrostatic interactions. Therefore, there is a real possibility that two ice particles come into contact and adhere due to electrical forces generated by different charge distributions or dipole interactions between their surfaces; even in the case that both particles can be electrically neutral as in the case of the droplets produced by condensation. Certainly, the probability of collision and adhesion will be enhanced if the particles are charged, as in the case of the droplets generated by the ultrasonic nebulizer. We can assume that each one of the nebulized droplets with enough electric charge produce an attractive force to a neighbor neutral droplet, due to the interaction between the droplet charge and the electric dipole induced on the neutral droplet. Schlamp et al. (1979) found that the collision efficiency between droplets of about 20 μm in diameter charged with $5 \times 10^{-8}$ esu (~100 elementary charges) of opposite sign may be raised by more than 30% respect to uncharged droplets. They concluded that in the absence of an external electric field, electric charges of opposite sign residing on drops invariably raise the collision efficiency of the drops with the increase most pronounced for the smallest drops. These results are also in agreement with the results reported by Latham and Saunders (1967) who found that crystal aggregation can be markedly enhanced if the cloud is highly electrified.

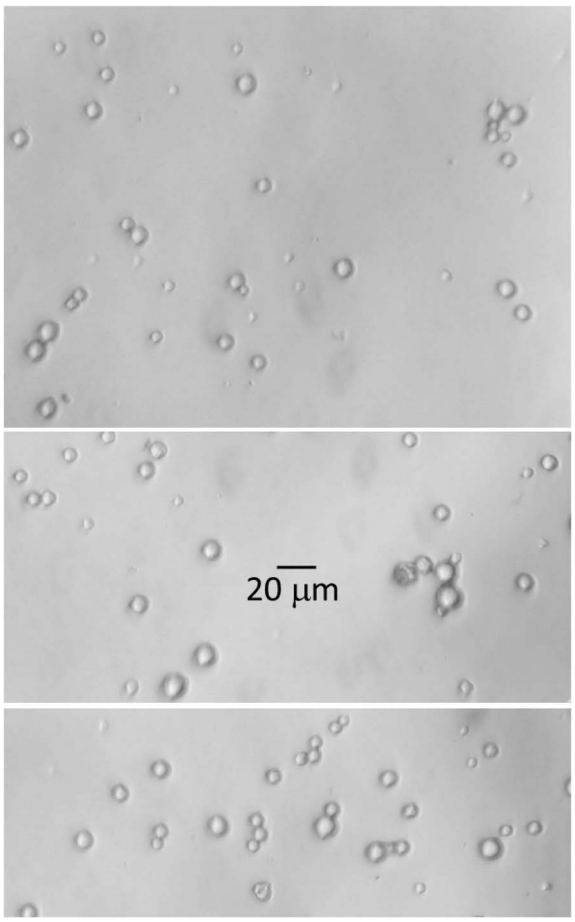


**Figure 5.** Images of collected cloud particles generated by an ultrasonic nebulizer.

Actually, aggregation of frozen droplets in nature should occur in presence of electric fields ($E$) rather than by charging of drops (Saunders & Wahab, 1975). In highly electrified thunderstorms, the electric field can induce dipoles on the droplets that can favor the aggregation mechanism through dipole-dipole interactions between neighboring droplets, similar to what happens with the charged frozen droplets in our experiments.

In order to analyze whether or not the aggregation process occurs with preferential or selected droplet sizes, a comparison between the droplet size distribution of single and aggregated droplets was performed. Figure 6 displays the size distribution of the single frozen droplets (Figure 6a) and the size distribution of the individual frozen droplets in the aggregates (Figure 6b) for cloud droplets formed by vapor condensation. Droplets aggregated with ice crystals were also considered in this

**Table 1**
*The Temperature Range (T), the Initial Concentration of Droplets ($C_o$), the Number of Single Frozen Droplets and the Number of Aggregates With 2, 3, 4, and >4 Droplets Counted in Each Experiment Performed With the Ultrasonic Nebulizer and With Water Condensation*

| Method | $T$ (°C) | $C_o$ (particle/L) | Single droplets | Two droplets aggregates | Three droplets aggregates | Four droplets aggregates | >4 droplets aggregates |
|---|---|---|---|---|---|---|---|
| Condensation | −(46 ± 1) | (70 ± 20)$10^3$ | 557 | 34 | 3 | 1 | 2 |
| Nebulization | −(43 ± 1) | (60 ± 20)$10^3$ | 374 | 70 | 25 | 8 | 16 |

analysis, in order to have a larger number of droplets. The same comparison was made for droplets formed by the ultrasonic nebulizer (Figures 6c and 6d). The existence of statistically significant differences between the size distribution of the single frozen droplets and the individual frozen droplets in the aggregates was determined with the chi-square test with a significance degree $p < 0.05$.

The size distribution of frozen droplets formed by the nebulizer and undergoing the aggregation process has more than 45% of droplets <6 μm, while the percentage of single frozen droplets <6 μm is less than 28%. Similarly, the size distribution of frozen droplets formed by condensation and undergoing the aggregation process has about 30% of droplets <6 μm, while the percentage of single frozen droplets <6 μm is less than 20%. These results suggest that the size distribution of frozen droplets undergoing the aggregation process has a larger proportion of small droplets (<6 μm) than the size distribution of the single frozen droplets, both for droplets formed by condensation and for droplets formed by the nebulizer. The average droplet diameters calculated in each case confirm this trend. In fact, the mean droplet diameter of single frozen droplets for droplets formed by vapor condensation and nebulizer were 9.0 μm and 7.4 μm, respectively, while the mean droplet diameter of aggregate droplets formed by vapor condensation and nebulizer were 8.2 μm and 6.6 μm, respectively. This result could be a consequence of the process of collision and adhesion conducted by electrical forces, which may be improved for smaller and lighter frozen droplets.

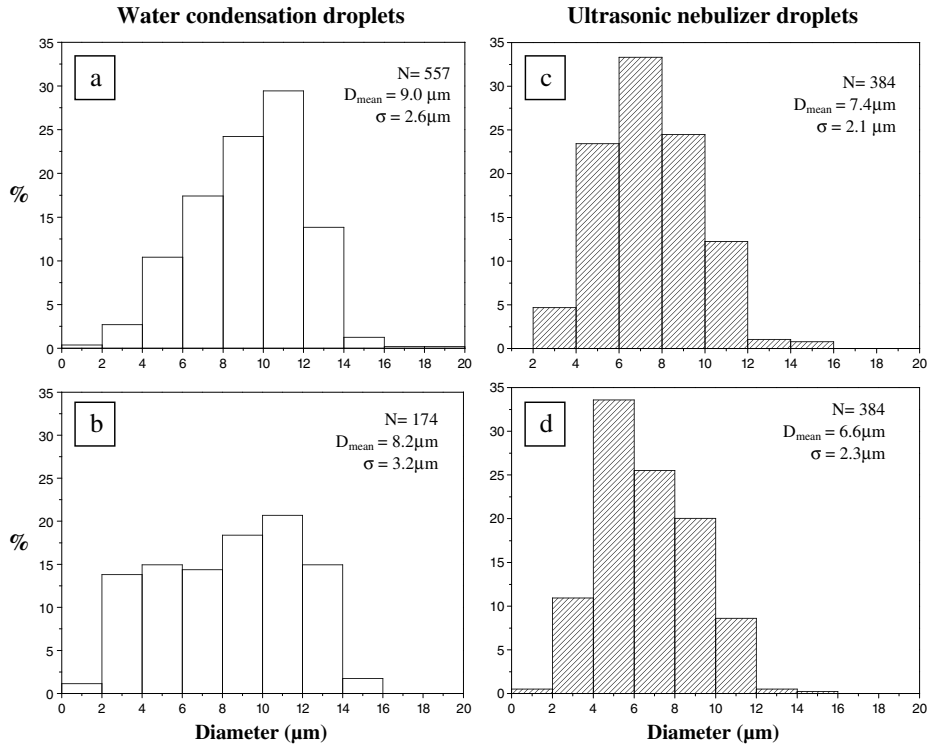


**Figure 6.** Size distribution of (a) single cloud droplets formed by condensation of water vapor. (b) Aggregated frozen droplets formed by vapor condensation. (c) Single cloud droplets formed by ultrasonic nebulizer. (d) Aggregated frozen droplets formed by ultrasonic nebulizer.

## 4. Summary and Concluding Remarks

This study reports laboratory measurements of the onset of the aggregation process of frozen droplets. The experiments were carried out for temperatures $< -40$°C, where the pure water droplets freeze spontaneously without the need for INPs. It was found that the aggregation process can occur for frozen droplet sizes around 10 $\mu$m in diameter and at concentrations of 70 $\pm$ 20 cm$^{-3}$, particle concentrations this high can be found in some regions of anvil cirrus. Studies of the aggregation process of frozen droplets are important, because it involves an enhancement of the growth rates and sedimentation of the particles, which play a key role on the lifetime of clouds that reside high in the troposphere.

Subsidiary experiments performed with electrically charged droplets show that the aggregation processes can be significantly improved, suggesting that the mechanism of collision and adhesion could be related to electrical forces generated by different charge distributions or dipole interactions between the interacting ice surfaces. It was observed that the aggregation process preferentially involves small frozen droplets, consistently with the idea that the electrical forces lead the process of collision and adhesion.

The current work aims at advancing our fundamental understanding of the aggregation process of frozen droplets, which is necessary for understanding the cloud microphysical processes and for climate modeling.

**Acknowledgments**
We thank Secretaría de Ciencia y Tecnología de la Universidad Nacional de Córdoba (UNC), Consejo Nacional de Investigaciones Científicas y Tecnológicas (CONICET), and Agencia Nacional de Promoción Científica (PICT 2015 2644) for their support. The raw data used to generate Figures 1–6 and Table 1 are included as supporting information. We thank María Laura López and José Barcelona for technical assistance.

## References

Allee, P. A., & Philips, B. B. (1959). Measurements of cloud-droplet charge, electric field, and polar conductivities in supercooled clouds. *Journal of Meteorology*, *16*(4), 405–410. https://doi.org/10.1175/1520-0469(1959)016%3C0405:MOCDCE%3E2.0.CO;2

Bailey, A. G., Hashish, A. H., & Williams, T. J. (1998). Drug delivery by inhalation of charged particles. *Journal of Electrostatics*, *44*(1-2), 3–10. https://doi.org/10.1016/S0304-3886(98)00017-5

Chow, H. Y., & Mercer, T. T. (1971). Charges on droplets produced by atomization of solutions. *American Industrial Hygiene Association Journal*, *32*(4), 247–255. https://doi.org/10.1080/0002889718506445

Connolly, P. J., Saunders, C. P. R., Gallagher, M. W., Bower, K. N., Flynn, M. J., Choularton, T. W., … Lawson, R. P. (2005). Aircraft observations of the influence of electric fields on the aggregation of ice crystals. *Quarterly Journal of the Royal Meteorological Society*, *131*(608), 1695–1712. https://doi.org/10.1256/qj.03.217

Gayet, J. F., Mioche, G., Bugliaro, L., Protat, A., Minikin, A., Wirth, M., … Gourbeyre, C. (2012). On the observation of unusual high concentration of small chain-like aggregate ice crystals and large ice water contents near the top of a deep convective cloud during the CIRCLE-2 experiment. *Atmospheric Chemistry and Physics*, *12*(2), 727–744. https://doi.org/10.5194/acp-12-727-2012

Heymsfield, A. J. (1986). Ice particle evolution in the anvil of a severe thunderstorm during CCOPE. *Journal of the Atmospheric Sciences*, *43*(21), 2463–2478. https://doi.org/10.1175/1520-0469(1986)043%3C2463:IPEITA%3E2.0.CO;2

Heymsfield, A. J., Miloshevich, L. M., Schmitt, C., Bansemer, A., Twohy, C., Poellot, M. R., … Gerber, H. (2005). Homogeneous ice nucleation in subtropical and tropical convection and its influence on cirrus anvil microphysics. *Journal of the Atmospheric Sciences*, *62*(1), 41–64. https://doi.org/10.1175/JAS-3360.1

Heymsfield, A. J., Bansemer, A., Durden, S. L., Herman, R. L., & Bui, T. P. (2006). Ice microphysics observations in Hurricane Humberto: Comparison with non-hurricane-generated ice cloud layers. *Journal of the Atmospheric Sciences*, *63*(1), 288–308. https://doi.org/10.1175/JAS3603.1

Heymsfield, A. J., Bansemer, A., Heymsfield, G., & Fierro, A. O. (2009). Microphysics of maritime tropical convective updrafts at temperatures from $-20°$ to $-60°$. *Journal of the Atmospheric Sciences*, *66*(12), 3530–3562. https://doi.org/10.1175/2009JAS3107.1

Hobbs, P. V., & Mason, B. J. (1964). The sintering and adhesion of ice. *Philosophical Magazine*, *9*(98), 181–197. https://doi.org/10.1080/14786436408229184

Hosler, C. L., Jensen, D. C., & Goldshlak, L. (1957). On the aggregation of ice crystals to form show. *Journal of Meteorology*, *14*(5), 415–420. https://doi.org/10.1175/1520-0469(1957)014%3C0415:OTAOIC%3E2.0.CO;2

Jensen, E. J., Lawson, P., Baker, B., Pilson, B., Mo, Q., Heymsfield, A. J., … Tanelli, S. (2009). On the importance of small ice crystals in tropical anvil cirrus. *Atmospheric Chemistry and Physics*, *9*(15), 5519–5537. https://doi.org/10.5194/acp-9-5519-2009

Johnson, D. A., & Hallett, J. (1968). Freezing and shattering of supercooled water drops. *Quarterly Journal of the Royal Meteorological Society*, *94*(402), 468–482. https://doi.org/10.1002/qj.49709440204

Kajikawa, M., & Heymsfield, A. J. (1989). Aggregation of ice crystals in cirrus. *Journal of the Atmospheric Sciences*, *46*(20), 3108–3121. https://doi.org/10.1175/1520-0469(1989)046%3C3108:AOICIC%3E2.0.CO;2

Kikuchi, K. (1972). Sintering phenomenon of frozen cloud particles observed at Syowa Station, Antarctica. *Journal of the Meteorological Society of Japan*, *50*(2), 131–135. https://doi.org/10.2151/jmsj1965.50.2_131

Knollenberg, R. G., Kelly, K., & Wilson, J. C. (1993). Measurements of high number densities of ice crystals in the tops of tropical cumulonimbus. *Journal of Geophysical Research*, *98*(D5), 8639–8664. https://doi.org/10.1029/92JD02525

Kumai, M. (1966). Electron microscopic study of ice-fog and ice-crystal nuclei in Alaska. *Journal of the Meteorological Society of Japan*, *44*(3), 185–194. https://doi.org/10.2151/jmsj1965.44.3_185

Latham, J., & Saunders, C. P. R. (1967). The adhesion of ice spheres in electric fields. *Journal of Glaciology*, *6*(46), 505–514. https://doi.org/10.1017/S0022143000019729

Lawson, R. P., Baker, B. A., & Pilson, B. L. (2003). In-situ measurements of microphysical properties of mid-latitude and anvil cirrus, proceedings, 30th international symposium on remote sensing of environment, Honolulu, Hawaii, November, 707–710.

Lawson, R. P., Jensen, E., Mitchell, D. L., Baker, B., Mo, Q., & Pilson, B. L. (2010). Microphysical and radiative properties of tropical clouds investigated in TC4 and NAMMA. *Journal of Geophysical Research*, *115*, D00J08. https://doi.org/10.1029/2009JD013017

Liou, K. (1986). Influence of cirrus clouds on weather and climate processes: A global perspective. *Monthly Weather Review*, *114*(6), 1167–1199. https://doi.org/10.1175/1520-0493(1986)114%3C1167:IOCCOW%3E2.0.CO;2

Lynch, D. K., Sasse, K., Starr, D. O. C., & Stephens, G. (2002). *Cirrus*. Oxford, UK: Oxford University Press.

Rosenfeld, D., & Woodley, W. L. (2000). Deep convective clouds with sustained supercooled liquid water down to −37.5°C. *Nature*, *405*(6785), 440–442. https://doi.org/10.1038/35013030

Rosenfeld, D., Woodley, W. L., Krauss, T. W., & Makitov, V. (2006). Aircraft microphysical documentation from cloud base to anvils of hailstorm feeder clouds in Argentina. *Journal of Applied Meteorology and Climatology*, *45*(9), 1261–1281. https://doi.org/10.1175/JAM2403.1

Saini, D., Biris, A. S., Srirama, P. K., & Mazumder, M. K. (2007). Particle size and charge distribution analysis of pharmaceutical aerosols generated by inhalers. *Pharmaceutical Development and Technology*, *12*(1), 35–41. https://doi.org/10.1080/10837450601166536

Salby, M. L., Hendon, H. H., Woodberry, K., & Tanaka, K. (1991). Analysis of global cloud imagery from multiple satellites. *Bulletin of the American Meteorological Society*, *72*(4), 467–480. https://doi.org/10.1175/1520-0477(1991)072%3C0467:AOGCIF%3E2.0.CO;2

Sassen, K., Wang, Z., & Liu, D. (2008). Global distribution of cirrus clouds from CloudSat/Cloud-Aerosol Lidar and Infrared Pathfinder Satellite Observations (CALIPSO) measurements. *Journal of Geophysical Research*, *113*, D00A12. https://doi.org/10.1029/2008JD009972

Saunders, C. P. R., & Wahab, N. M. A. (1975). The influence of electric fields on the aggregation of ice crystals. *Journal of the Meteorological Society of Japan*, *53*(2), 121–126. https://doi.org/10.2151/jmsj1965.53.2_121

Schaefer, V. J. (1956). The preparation of snow crystal replicas—VI. *Weatherwise*, *9*(4), 132–135. https://doi.org/10.1080/00431672.1956.9927220

Schlamp, R. J., Grover, S. N., & Pruppacher, H. R. (1979). A numerical investigation of the effect of electric charges and vertical external electric fields on the collision efficiency of cloud drops: Part II. *Journal of the Atmospheric Sciences*, *36*(2), 339–349. https://doi.org/10.1175/1520-0469(1979)036%3C0339:ANIOTE%3E2.0.CO;2

Schmitt, C. G., Stuefer, M., Heymsfield, A. J., & Kim, C. K. (2013). The microphysical properties of ice fog measured in urban environments of interior Alaska. *Journal of Geophysical Research: Atmospheres*, *118*, 11,136–11,147. https://doi.org/10.1002/jgrd.50822

Stith, J. L., Avallone, L. M., Bansemer, A., Basarab, B., Dorsi, S. W., Fuchs, B., … Toohey, D. W. (2014). Ice particles in the upper anvil regions of midlatitude continental thunderstorms: The case for frozen-drop aggregates. *Atmospheric Chemistry and Physics*, *14*(4), 1973–1985. https://doi.org/10.5194/acp-14-1973-2014

Thuman, W. C., & Robinson, E. (1954). Studies of Alaskan ice-fog particles. *Journal of Meteorology*, *11*(2), 151–156. https://doi.org/10.1175/1520-0469(1954)011%3C0151:SOAIFP%3E2.0.CO;2